Leveraging the flexibility of electric vehicle parking lots in distribution networks with high renewable penetration

Sahand Karimi-Arpanahi[a,*], Mohammad Jooshaki[b], S. Ali Pourmousavi[a], Matti Lehtonen[c]

[a]*School of Electrical and Electronic Engineering, University of Adelaide, Adelaide, SA 5005, Australia*
[b]*Circular Economy Solutions Unit, Geologian Tutkimuskeskus (GTK), Espoo, FI-02151, Finland*
[c]*Department of Electrical Engineering and Automation, Aalto University, Espoo, FI-02150, Finland*

Abstract

The ongoing rapid increase in the integration of variable and uncertain renewable energy sources calls for enhancing the ways of providing flexibility to power grids. To this end, we propose an optimal approach for utilizing electric vehicle parking lots to provide flexibility at the distribution level. Accordingly, we present a day-ahead scheduling model for distribution system operators, where they can offer discounts on the network tariff to electric vehicle parking lot operators. This way, they will be encouraged to exploit the potential flexibility of electric vehicle batteries to assist in alleviating the steep ramps of system net-load. To determine the optimal discounts, the distribution system operator minimizes the network operating costs considering the network operational constraints, while the electric vehicle parking lot operators try to maximize their profits. Due to the contradictory objectives and decision hierarchy, the problem is an instance of Stackelberg games and can be formulated as a bi-level program, which is linearized and converted to a single-level mixed-integer linear program using strong-duality theorem and Karush-Kuhn-Tucker conditions. To validate the proposed model, comprehensive simulation studies are performed on a test distribution network. The simulation results show that implementing the model can reduce the peak-off-peak difference and peak-to-average ratio of the network net-load by up to 15% and 24%, respectively.

Keywords: Bi-level programming, Distribution network operation, Electric vehicle parking lot, High renewable energy, Power system flexibility

Nomenclature

Superscripts

arr/dep	PEV arrival/departure to/from the EVPL.
ch/dch	Electric vehicle battery charging/discharging.
CD	Conventional demand.
deg	PEV battery degradation.
des/ini	Desired/initial PEV battery state-of-charge.
DG	Renewable distributed generation source.
EV	Plug-in electric vehicle.
LN	Distribution network line.
min/max	Minimum/maximum value.
nom	Nominal value.
PL	Electric vehicle parking lot.
pw	Piecewise linear function.
sqr	Squared value.
SS	Distribution network substation.
WE	Wholesale energy market.

Indices

i	Index for the PEVs parked in an EVPL.
l	Index for sigma points.
m,n,k	Indices for load nodes.
mn	Index for the line connecting nodes m and n.
pc, q	Indices for segments of the piecewise linear function.
s	Index for discount steps.
ss	Index for substations.
t	Index for time intervals.

Sets

E	Set of nodes where EVPLs are located ($E \subseteq N$).
H	Set of time intervals during a day.
I_n	Set of PEVs in the EVPL located at node n.
L	Set of distribution network lines.
N	Set of distribution network nodes.
PC	Set of segments of the piecewise linear function.
S	Set of discount steps.
TR	Set of substations.

Parameters and Variables

A	Size of each segment of the piecewise linear function.
BC/BP	Battery capacity/price of PEVs.
ce	Curtailed RES generation.
D	Amount of discount on network tariff.

*Corresponding author
Email address: sahand.karimi-arpanahi@adelaide.edu.au (Sahand Karimi-Arpanahi)

EoL	PEV battery end-of-life threshold in percentage.
fl	Current of distribution network lines.
K	Slope of each segment of the piecewise linear function.
O	Number of random variables.
pr	Profit of EVPLs.
$P, p/Q, q$	Active/reactive power.
R, X, Z	Resistance, reactance, and impedance of lines.
RU/RD	Net-load ramp-up/down penalty in each interval.
r^+/r^-	Positive/negative ramp rate of network net-load.
sc	State-of-charge of PEV batteries.
SC	Substation capacity.
T	PEV battery temperature.
u	Segment of the piecewise linear function.
V, v	Voltage of distribution network nodes.
W	Weight associated with each sigma point.
Y	Output vector of the SSUT.
Z	Input vector of the SSUT (random variables).
δ	Binary variable indicating if the DSO gives discount on network tariff.
Δt	Length of a time interval.
η	PEV battery charging/discharging efficiency.
λ/μ	Dual variables of equality/inequality constraints.
Π	Electrical energy price.
χ^j	j-dimensional spherical simplex sigma point set.

1. Introduction

1.1. Motivation

The realization of global climate change has initiated an orchestrated global effort to produce electricity from green energy resources and to electrify the transportation sector. As a result, financial incentives and regulatory policies [1, 2] are developed, which have accelerated the grid integration of renewable energy sources (RESs) and the use of plug-in electric vehicles (PEVs). In addition, the adoption of the new technologies has been exacerbated by the ever-decreasing cost of RESs and storage technologies in the past few years [2]. The recent commitment of more than 40 countries at the COP26 climate summit to phase out coal power plants will also accelerate the current rate of RES integration into power grids [3].

While these low-carbon technologies offer a plethora of environmental and economic benefits, they may lead to several challenges in the power grid operation [4]. A fundamental challenge is to effectively deal with the volatile and uncertain nature of RES generation and uncoordinated PEV charging in order to manage their impacts on grid stability and reliability [5]. In highly RES-penetrated power grids, steep ramping events are common. These may cause significant momentary imbalances between demand and supply [6], which can threaten the power system stability. In general, steep ramps may lead to significant RES curtailment, power balance violation in a control area, negative market prices, and price volatility in power grids [7].

Traditionally, grid operators relied on synchronous generators to manage the imbalance between demand and supply in different time scales [8]. However, even if the possibility of congestion at the transmission system is disregarded, the integration of RESs together with the retirement of conventional synchronous power plants intensifies the issues related to generation and demand balance. Thus, it is crucial to develop strategies to provide more flexibility sources for power grid operation and to ensure supply-demand balance at a reasonable cost. While new market products have been proposed to facilitate the utilization of new flexibility sources, managed at the transmission level, distribution system operators (DSOs) can be encouraged to provide flexibility in their corresponding networks by developing innovative methods [9]. Such flexibility sources at the distribution level can fulfill the requirements more efficiently, as they can eliminate the need for costly investments in the generation and transmission sectors [6, 9].

Due to the natural monopoly in the electricity distribution business, national regulatory authorities (NRAs) may incentivize DSOs to improve service quality, cost efficiency, security of supply and other similar services through new regulations [10]. As previously discussed, the steep ramping events, caused by large amounts of RESs in the grid, may not only threaten the power grid stability but also can lead to higher prices in the regulation market, which essentially increases the electricity costs for the end-users. Aiming at motivating DSOs to alleviate the steep ramps at the distribution level, NRAs can impose appropriate regulations on DSOs. The authors in [11] proposed several policies for this purpose and considered dispatchable distributed generation (DG) units and energy storage systems as the available flexibility resources that can be used by DSOs. While such resources can be cost-effective in some applications, they might be considered too costly in others. Thus, a more efficient approach is to utilize the available flexibility resources in distribution networks (DNs) to avoid or defer further investments. In this regard, PEV parking lots (EVPLs), which are often privately-owned and their operators aim to maximize their profit, can be considered as a source of flexibility contingent on developing enabling schemes.

1.2. Related Works

In recent years, many methods have been proposed to exploit the potential of PEVs in providing different types of services to the DN. The authors in [12] proposed a novel algorithm for EV charging scheduling with the goal of improving supply voltages along a distribution feeder. In [13], an operational model for distribution companies (DISCOs) was proposed to reduce the DN operation costs by shifting the PEV aggregator (EVA) demand to periods with

lower electricity prices. Also, the authors in [14] proposed a scheduling model for DN operation, where PEVs could be utilized for load curtailment services to smooth the net exchanged power fluctuations caused by RESs. Nonetheless, the authors in [12–14] developed the scheduling models for PEV charging plan or DN operation without acknowledging the interactions between different agents in the DN, e.g., DSO-EVAs or DSO-EVPLs. Additionally, while the models proposed in [12–14] can be used for providing the aforementioned services to the DN, they may not be adapted for enhancing the flexibility of the DN, i.e., minimizing the net-load ramp rate.

Another group of researchers have specifically focused on leveraging the EVAs for providing services for the DN operation. In this regard, the authors in [15] and [16] considered the interactions between the DSO and the EVAs by developing distribution locational marginal pricing (DLMP)-based methods to motivate the EVAs to participate in managing congestion at DNs. For instance, Huang *et al.* in [16] developed a bi-level model that minimizes the cost of the DSO in the upper-level and that of the aggregators of PEVs and heat pumps in the lower-level along with a dynamic subsidy method for DN congestion management. Although the proposed approaches in those studies presented effective methods for providing services to the DN via EVAs, they did not investigate the potential of EVPLs for providing services to DNs [15, 16]. In addition, such studies have focused on market-based approaches at the distribution level to incentivize the EVAs to provide services. However, implementing such schemes requires local electricity markets, which seems pretty far-fetched [9]. In addition, it would be better to motivate EVPLs to provide services (in our case, flexibility) that benefits the DN operation without a market-based approach, in an attempt to avoid complexities in the DSO's operation. Finally, none of the models proposed in these studies can be adapted to provide flexibility to the DN since they are developed for DN congestion management.

Given the growth of privately-owned EVPLs in recent years, several studies have developed frameworks for efficiently integrating them into power grids. In this regard, the authors in [17] presented a smart EV charging scheme to reduce electricity and charging infrastructure costs associated with workplace EVPLs. Also, Neyestani *et al.* in [18] introduced a framework for the interactions of EVPLs with the energy and reserve markets via an EVA. In [19], the authors proposed an approach for the participation of EVPLs in multiple electricity markets, aiming at maximizing the EVPLs' profit as well as minimizing the DSO operation cost. In [20], the authors proposed a bi-level program for modeling the interactions between the DSO and the EVPLs, aiming at minimizing the costs of both entities. Conceptually similar to the bi-level model in [20], the authors in [21] presented an operational scheduling model for distribution companies in the presence of RESs and EVPLs to minimize the utilities' cost and maximize the EVPLs' profit. Despite the efforts made in [17–21], the proposed methods do not offer mechanisms to encourage EVPL operators to provide any specific services to the DN. Authors in [22] presented two charging strategies for workplace parking lots, aiming at either minimizing the charging cost or minimizing the peak-to-average ratio (PAR). However, the impact of the proposed strategies on the DN operation was overlooked, and no cost-benefit analysis has been performed to assess the efficiency of the proposed model. The cost-benefit study is important because a rational EVPL operator will not provide services to DNs unless extra profit can be envisaged.

In addition to the identified knowledge gaps in the literature, to the best of our knowledge, no previous research has proposed an approach for flexibility provision at the distribution level (i.e., minimizing the net-load ramps of the DN) through EVPLs/EVAs. Moreover, while a simplified version of the linearized AC optimal power flow (OPF) is employed in [12, 16, 19, 21], the models in [18, 20] did not consider any OPF formulations, which fails to guarantee the feasibility of the results. Also, the approaches proposed in [12, 14–22] did not consider the uncertainty associated with RES generation, EVPL load, and conventional loads. This issue is critical in a network with high RES penetration and PEV demand since their day-ahead forecast might have considerable errors. Additionally, the costs related to the PEV battery degradation were not considered in [14–17, 20]; also, the battery degradation models that were used in [13, 18, 19, 21, 22] did not account for the impact of the charge and discharge power on the PEV battery degradation. Such simplistic degradation models are not suitable for the applications in which the PEVs are utilized to provide various services to the DN as the services should be monetized accurately. Using a simple battery degradation model may lead to over- or under-estimation of EVPLs' cost and thus flexibility.

1.3. Objectives and Contributions

Addressing the issues discussed previously, this paper proposes a framework that enables the DSO to exploit the EVPLs flexibility at the distribution level. To this end, we develop a mathematical model for day-ahead scheduling of DNs with high penetration of PEVs and RESs by providing mechanisms to facilitate EVPLs participation in flexibility provision. In the proposed framework, the DSO aims at minimizing the DN operating costs, while alleviating the network net-load ramps using the flexibility of PEVs parked in the EVPLs. The operational constraints of the DN are considered in the problem using an accurate linear AC OPF model to ensure that the DN operation is technically feasible. Also, the prediction uncertainties of RES generation, EVPL demand, and conventional loads are taken into account through an efficient analytical uncertainty modeling technique, i.e., spherical simplex unscented transformation (SSUT).

The main objective of each EVPL operator is to maximize its own profit. As a result, they have no tendency

Table 1: Comparison of the proposed model with the most relevant studies

Ref.	Stakeholders		Accurate PEV Battery Degradation	DN Technical Constraints	Correlated RES and Demand Uncertainties	Unfixed Energy Price and Plan for EVAs/EVPLs [a]	LP/MILP Optimization [b]
	Upper-Level	Lower-Level					
[12]	Single-Level		✓	✓	✗	✗	✗
[13]	Single-Level		✗	✓	✓	✗	✓
[14]	Single-Level		✗	✓	✗	✗	✗
[16]	DSO	Aggregator	✗	✓	✗	✗	✓
[18]	Aggregator	EVPL/DG/Retailer	✗	✗	✗	✗	✓
[19]	Two-Level (DSO and EVPL) [c]		✗	✓	✗	✗	✓
[21]	DISCO	EVPL	✗	✓	✗	✗	✓
This paper	DSO	EVPL	✓	✓	✓	✓	✓

[a]: Both the price and amount of the energy consumed by EVs are variables, determined by solving the optimization.
[b]: MILP models can be solved by commercial solvers with a guaranteed convergence to a globally optimal solution.
[c]: The "two-level" optimization, where the problems of both levels are solved simultaneously, is different from bi-level.

to support the DSO by providing flexibility unless financial incentives are provided, e.g., discounts on the network tariffs in specific time intervals during a day. Considering the discounted network tariffs, the EVPL operators will reschedule the charging of PEVs, aiming at increasing their profit. The EVPL may also exploit the vehicle-to-grid (V2G) operation of PEVs to increase their profit. Since the objectives of the DSO and EVPLs are contradictory, a bi-level optimization problem is formulated where the decision-making process of the DSO and the EVPLs is considered at the upper- and lower-level, respectively. The network tariff discounts are determined by the proposed optimization problem such that the rescheduled charging pattern of EVPLs provides adequate flexibility to the DN. This way, not only does the profit of each EVPL increase due to the discounted network tariffs, but also the DSO leverages the flexibility of PEVs parked in the EVPLs to smooth the DN net-load. To avoid overestimating the flexibility from EVPLs, an accurate battery degradation model is adapted in this paper by considering the impact of PEV battery charging/discharging rates on its degradation.

It is worth noting that the bi-level models proposed for modeling the interaction of the DSO (in the upper-level) and the EVAs/EVPLs (in the lower-level) in the previous studies, e.g., [16] and [21], have assumed that either the price or the amount of EVA/EVPL consumed energy at each time interval is constant in the equivalent single-level problems in order to avoid computational complexities of multiplication of two decision variables. However, we have avoided making such simplifications in our bi-level problem to accurately model the system. After linearizing the nonlinear equations in the bi-level problem, we converted it into an equivalent single-level mixed-integer linear programming (MILP) problem, which can be solved with guaranteed convergence to global optimality. In summary, the main contributions of this paper are as follows:

- Proposing a framework for the DSO to exploit the potential flexibility of EVPLs for smoothing the DN net-load and developing a mathematical model for this purpose, where the interactions between the DSO and EVPL operators are modeled.
- Devising a MILP problem to optimize the discounts on the network tariffs offered by DSOs to EVPLs in order to motivate them to provide services to the DN (in this paper, to enhance the distribution network flexibility).
- Developing a linear model for estimating the degradation cost of PEV batteries caused by the EVPLs' providing services to the DN, which considers the impact of charging/discharging current on the marginal battery degradation cost.

In addition to the main contributions of this article, Table 1 summarizes the differences between the proposed model and the most relevant research studies in the field. In the table, symbols "✓" and "✗" indicate if a particular feature is considered or not, respectively.

1.4. Paper Structure

The rest of this paper is organized as follows. After introducing the proposed framework in Section 2, the mathematical formulation of the corresponding bi-level problem is presented in Section 3. We then explain how the uncertainties are considered in Section 4. Also, the methods used for converting the nonlinear bi-level problem into a single-level MILP model are presented in Section 5. We show the effectiveness of our model and justify the claimed contributions in Section 6. Finally, Section 7 concludes the paper.

2. Proposed Framework

This section presents the general framework of the proposed model for the DSO day-ahead scheduling. It is known that the EVPL operators manage the charging of the parked PEVs in order to maximize their profits, considering PEV users' constraints and preferences. As it was

argued in the Introduction, EVPLs can provide flexibility when lucrative incentives are provided by the DSO. Such financial incentives could be in the form of discounts on network tariffs. This way, the DSO does not need to engage in energy markets. Rather, a discount on the network tariff is offered to the EVPLs by the DSO during some time intervals. Such discounts would be compliant with the NRAs' regulations as they would fall within the framework of the performance-based regulations for distribution companies [23–25]. Under such regulatory regimes, DSOs have the flexibility to offer discounted prices to their customers as long as they meet the regulated price or revenue cap. In the proposed framework in this paper, the DSO incentive is only in the form of a discount. Therefore, the network tariff will never exceed the original value. Note that the network tariff is a percentage of the energy price that EVPLs or other electricity consumers pay. Thus, the DSO can only provide discount on its own share of the electricity price of the end-users. This approach is better than implementing dynamic tariffs on the use-of-network charges as it may raise a number of problems. On the one hand, frequently changing the network usage fees is not compliant with the "good" regulatory practices [26]. On the other hand, one network tariff structure is typically designed for all end-users or a few specific types of customers, e.g., residential, commercial, and industrial. Thus, a tariff structure is not flexible enough to be tailored for specific users like EVPLs. Accordingly, instead of designing a completely different use-of-system tariff structure, we propose minimally adjusting the tariffs by offering limited discounts. Aside from the aforementioned limitations, the proposed discount-based approach is conceptually similar to the incentive-based demand response programs, while varying network tariffs might be regarded as a price-based program. Incentive-based programs feature higher flexibility to improve the system operation during specific events. Also, note that, in the proposed framework, the discount is offered to the EVPL operators, not the PEV owners; thus changing the behavior of end-users, which can lead to various difficulties in the practical implementation of the model, is not required.

Aiming at determining the amount of tariff discounts in each time interval, the DSO needs to conduct day-ahead scheduling to estimate EVPL consumption in the presence of the discounts. The DSO specifies the network tariff discounts for each of the EVPLs exclusively so as to encourage the corresponding EVPL operator to utilize the flexibility of parked PEVs. In this problem, the DSO wants to minimize its objective function (i.e., the network cost), while the EVPL operators' objective is to optimize their profit. Since the objectives of the DSO and EVPL operators are contradictory, considering the hierarchy of decision-making, this model is an instance of Stackelberg games. In this game, the DSO (leader) decides on the amount of discount on the network tariff and, afterward, the EVPL operators (followers) respond according to their own interests.

Such a Stackelberg game can be modeled as a bi-level optimization problem [27]. In this respect, in its upper-level problem, the DSO solves an operational scheduling problem for every interval of the next day to minimize its costs while satisfying network operational constraints, e.g., voltage and thermal constraints. It is assumed that the regulator has imposed a penalty-based policy on the DSO to encourage lower ramp rates in the DN [11]. As a result, the DSO tries to minimize the penalty by utilizing the potential flexibility of EVPLs for decreasing the DN net-load ramp rates. In each lower-level problem, however, an EVPL operator maximizes its profit, while satisfying technical constraints of charging facilities as well as PEVs' requirements. The discounts on the network charges are offered to the EVPL operators such that they would promote a change in the EVPLs charging profile.

The solution to the proposed bi-level optimization is the optimal network tariff discounts in each interval of the next day such that the total cost of DSO is minimized, while the operational constraints of the DN are satisfied. After obtaining the optimal solution, the DSO will broadcast the network tariff discounts to the EVPL operators. Therefore, each EVPL operator will manage the parked PEVs charging according to the discounted network tariffs, and the outcome will be a reduction in the ramp rates of DN net-load.

The proposed model is a nonlinear bi-level problem, which is not only difficult to solve, but also the solution convergence to the global optimum is not guaranteed. To address this issue, we firstly linearize the nonlinear terms of the AC OPF and the battery degradation equations in the upper-level problem. Then, we utilize Karush–Kuhn–Tucker (KKT) optimality conditions or the strong duality theorem to replace the lower-level problem with a set of constraints in the upper-level problem and cast the bi-level model as an equivalent mixed-integer nonlinear single-level problem [28]. Finally, the nonlinear terms in the objective functions of the DSO and the EVPL operators in the mixed-integer nonlinear problem will be linearized. The resulting MILP problem can be solved by a commercial solver to obtain the global optimal solution.

The flowchart represented in Fig. 2 shows the general structure of the proposed model, where the DSO solves an optimization problem to obtain the discounts, $\delta_{n,t,s}$, in the upper-level problem. Then, each EVPL operator maximizes its profit by determining the charging and discharging powers of PEVs, $P^{ch}_{n,i,t}$ and $P^{dch}_{n,i,t}$, based on the DSO's discounts. Hence, the charging and discharging powers of PEVs are decision variables for the corresponding EVPL operator, while they are considered as given parameters in the upper-level problem. Conversely, the discounts determined by the DSO in the upper-level are known parameters in the lower-level problems.

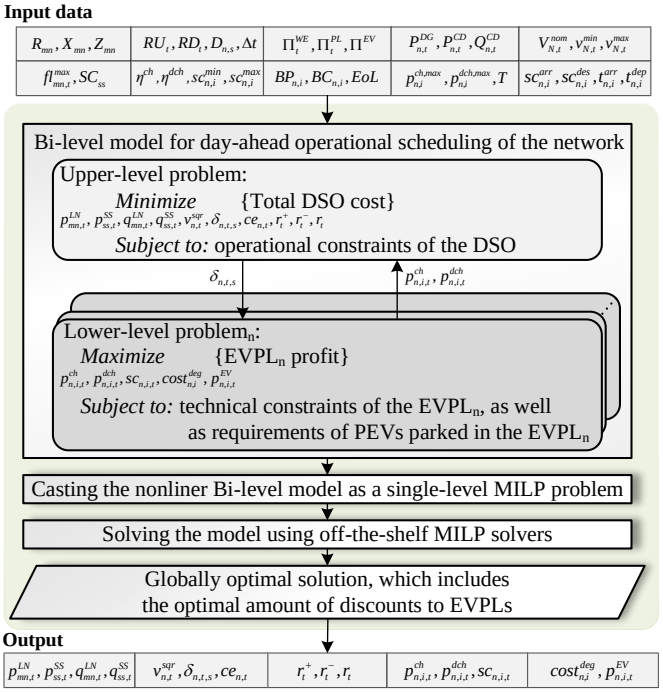

Figure 1: The flowchart of the proposed model.

3. Mathematical Formulation

In this section, the mathematical formulation of the proposed bi-level problem is presented in a deterministic form. As noted previously, the DSO is the leader, while the EVPL operators are the followers in the proposed bi-level problem. Thus, in the upper-level problem, the DSO minimizes its costs, while in each lower-level problem, an EVPL operator maximizes its profit. Please note that several followers may exist in the bi-level problem because various EVPLs might be connected to a DN.

3.1. Upper-Level Problem

Equation (1a) minimizes the objective function of the DSO, which is the total DN operating costs, including the cost of energy losses, $cost_{los}$, RES generation curtailment cost, $cost_{cur}$, flexibility-oriented cost, $cost_{flex}$, and the lost income due to the discounts offered to EVPLs, $cost_{dis}$. These costs are respectively formulated in the first, second, third, and fourth terms of the objective function, OF. The quadratic terms in the energy loss function, $cost_{los}$, are linearized through a piecewise linearization approach described in Subsection 5.1. The second term, $cost_{cur}$, is the financial losses due to curtailed RES generation that should be compensated by the DSO, and (1b) ensures that the curtailed generation is lower than the total generation of each RES in each interval. Also, similar to [11], ramp-ups and -downs of the DN net-load are penalized with respect to their slope. The penalty cost, $cost_{flex}$, is determined by calculating the amount of ramp-up, r_t^+, or ramp-down, r_t^-, in each interval, using (1c)–(1e). It is evident that only one of these two variables would have a non-zero value in each time interval, as the objective function is monotonically increasing with respect to each of them. Regarding $cost_{dis}$ in the objective function, the DSO may choose one of the discount steps in set S to reduce the network tariff for each of the EVPLs by that amount of discount in each interval. It is worth noting that the discount variables were originally continuous decision variables bounded within upper/lower constraints. However, the original optimization problem with continuous variables for the discounts is not tractable considering a zero optimality gap (i.e., the gap between the incumbent and the best bound of the global optimal solution) in the MILP problem. In addition, the applicability of the solution to the original problem (i.e., the optimal discounts) was severely sensitive to a non-zero optimality gap. As a result, we decided to use discrete variables for the discounts to obtain reliable, optimal solutions to the problem.

Lastly, the AC OPF is integrated into the model through (1g)–(1l). Active and reactive power balance is formulated in (1g) and (1h), respectively. While (1i) determines the voltage drop across line mn, (1j) ensures that the nodal voltages are within the upper and lower limits. The thermal constraints of lines and substation transformers are formulated in (1k) and (1l), respectively. Finally, equations (1g)–(1i), (1k), and (1l) are linearized by using the two-stage method discussed in Subsection 5.3.

$$\underset{\mathbf{\Phi}}{\text{Min}}\ OF = \Pi^{los}\sum_{mn\in L}\sum_{t\in H}\frac{R_{mn}((p^{LN}_{mn,t})^2+(q^{LN}_{mn,t})^2)}{(V^{nom}_{m,t})^2}\Delta t + \sum_{n\in N}\sum_{t\in H}\Pi^{WE}_t ce_{n,t} + \sum_{t\in H}(RU_t r^+_t + RD_t r^-_t)\Delta t + \sum_{n\in E}\sum_{i\in I_n}\sum_{t\in H}\sum_{s\in S} D_{n,s}\delta_{n,t,s}p^{ch}_{n,i,t}\Delta t \quad (1a)$$

Subject to:

$$0 \le ce_{n,t} \le P^{DG}_{n,t}; \forall n \in N, \forall t \in H \quad (1b)$$

$$r_t = \sum_{ss\in TR}(p^{SS}_{ss,t} - p^{SS}_{ss,t-1}); \forall t \in H \quad (1c)$$

$$r_t = r^+_t - r^-_t; \forall t \in H \quad (1d)$$

$$r^+_t, r^-_t \ge 0; \forall t \in H \quad (1e)$$

$$\sum_{s\in S}\delta_{n,t,s} \le 1; \forall n \in E, \forall t \in H \quad (1f)$$

$$\sum_{km\in L}\left[p^{LN}_{km,t} - \frac{R_{km}}{(V^{nom}_{k,t})^2}\left((p^{LN}_{km,t})^2 + (q^{LN}_{km,t})^2\right)\right] - \sum_{mn\in L} p^{LN}_{mn,t} = p^{SS}_{m,t} + P^{DG}_{m,t} - P^{CD}_{m,t} - \sum_{i\in I_m}(p^{ch}_{m,i,t} - p^{dch}_{m,i,t}) - ce_{m,t}; \forall m \in N, \forall t \in H \quad (1g)$$

$$\sum_{km\in L}\left[q^{LN}_{km,t} - \frac{X_{km}}{(V^{nom}_{k,t})^2}\left((p^{LN}_{km,t})^2 + (q^{LN}_{km,t})^2\right)\right] - \sum_{mn\in L} q^{LN}_{mn,t} = q^{SS}_{m,t} - Q^{CD}_{m,t}; \forall m \in N, \forall t \in H \quad (1h)$$

$$v^{sqr}_{m,t} - v^{sqr}_{n,t} = 2(R_{mn}p^{LN}_{mn,t} + X_{mn}q^{LN}_{mn,t}) + \frac{Z^2_{mn}}{(V^{nom}_{n,t})^2}\left((p^{LN}_{mn,t})^2 + (q^{LN}_{mn,t})^2\right); \forall mn \in L, \forall t \in H \quad (1i)$$

$$(v^{min}_{n,t})^2 \le v^{sqr}_{n,t} \le (v^{max}_{n,t})^2; \forall n \in N, \forall t \in H \quad (1j)$$

$$(p^{LN}_{mn,t})^2 + (q^{LN}_{mn,t})^2 \le v^{sqr}_{m,t}(fl^{max}_{mn})^2; \forall mn \in L, \forall t \in H \quad (1k)$$

$$(p^{SS}_{ss,t})^2 + (q^{SS}_{ss,t})^2 \le (SC_{ss})^2; \forall ss \in TR, \forall t \in H \quad (1l)$$

where $\mathbf{\Phi} = \{p^{LN}_{mn,t}, p^{SS}_{ss,t}, q^{LN}_{mn,t}, q^{SS}_{ss,t}, v^{sqr}_{n,t}, \delta_{n,t,s}, ce_{n,t}, r^{+}_{t}, r^{-}_{t}, r_t\}$ is the set of decision variables in the upper-level problem.

Evidently, the decision variables of the lower-level problems, i.e., PEV charging and discharging powers, $p^{ch}_{n,i,t}$ and $p^{dch}_{n,i,t}$, are considered parameters in the upper-level problem. However, as mentioned previously, we aim to recast this bi-level model as a single-level problem. As a result, a binary variable will be multiplied by a continuous variable in $cost_{dis}$ of (1a), which is a nonlinearity in the final single-level model. To address this issue, multiplication of a binary variable, a, and a continuous variable, b, can be equivalently modeled linearly as follows:

$$c \leq aM \tag{2a}$$
$$c \leq b \tag{2b}$$
$$c \geq b - (1-a)M \tag{2c}$$
$$c \geq 0 \tag{2d}$$

where M is a sufficiently large number, and c is an auxiliary continuous variable that is equal to the multiplication of a and b. Hence, by replacing the nonlinear term with c and adding the extra constraints, we will have a linear single-level optimization problem.

3.2. Lower-Level Problem

In each lower-level problem, an EVPL operator tries to maximize the profit obtained from charging PEV batteries, while fulfilling the technical constraints of PEVs and the need of PEV owners, as presented in (3). In this model, both V2G and grid-to-vehicle (G2V) operations are considered. The EVPL revenue comes from selling electricity to PEV owners and trading energy with the upper market through V2G services, whereas the costs are due to the consumed electricity during charging and the PEV battery degradation during V2G. As can be inferred from the objective function of the lower-level problem, (3a), the DSO's discounts on the network tariff would decrease the price of electricity for the EVPLs in some intervals of the day to facilitate higher electricity consumption in those intervals in comparison with the case with no discount. Please note that the binary variables in the upper-level problem, $\delta_{n,t,s}$, in (3a) do not make the lower-level problem nonlinear, as they are parameters in the lower-level. It is also worth noting that, in the objective function of the lower-level problem, we have assumed that all the profit will be for the EVPL, while the PEV owners only receive compensation from the EVPL for the battery degradation used by the EVPL to provide flexibility to the DN. Nevertheless, in a pre-defined shared profit arrangement where the EVPL receives a percentage of the profit, the objective function (profit) of the lower-level problem can be multiplied by that amount. This way, the optimal solution will not change as the problem is linear, although the profit amount would change. Hence, changing the distribution of the profit between the PEV owners and the EVPL will not change the optimal solution.

Since the source of flexibility is PEV batteries, it is essential to consider the impact of EVPLs' strategy during charging and V2G operation on the degradation of PEV batteries. To do so, a battery degradation model, inspired by the model in [29], is considered in the proposed problem, where the impact of temperature and charging-discharging current is considered on the battery degradation. This way, excessive battery charging-discharging regimes will be avoided, and PEV owners will be compensated for additional battery degradation due to the flexibility provision by the EVPL operators. Nevertheless, the battery degradation model proposed in this paper is linear, unlike [29], avoiding the introduction of nonlinear terms in the model. The cost of battery degradation is formulated in (3b)–(3d) for each PEV, which respectively determine the battery degradation cost due to V2G and G2V operation, the battery power exchange in each time slot, and the percentage of battery capacity loss caused by p_t at time t. In the proposed model, the EVPL operator only pays for the degradation cost caused by providing V2G and flexibility services. Thus, the degradation cost in a normal battery charging case is subtracted from the total battery degradation cost in (3b). Battery end of life is defined by an $EoL\%$ of reduction in its rated capacity. While the model used for determining the percentage of battery capacity loss in (3d) is highly accurate, the exponential function and multiplication of two decision variables in (3d) introduce nonlinearity in the formulation. Since the xe^x is a convex function for all $x > 0$, we may replace it with a piecewise linear function to linearly model the degradation cost. Please refer to Subsection 5.1 for more details regarding the piecewise linearization.

Equations (3e)–(3k) ensure that technical constraints of PEVs and PEV owners requirements are fulfilled. Each equation is succeeded by its corresponding dual variable, separated by a colon. The state-of-charge (SOC) of each PEV battery at each interval is calculated according to the charging/discharging power by (3e). Expressions (3f) and (3g) show the PEV battery charging and discharging power constraints. Equation (3h) ensures that the SOC of batteries are within the safe range. The initial SOC of each PEV battery is determined by (3i) at the beginning of the charging period, and the desired battery SOC before the PEV departure is enforced by (3j). Finally, (3k) ensures that PEVs are charged/discharged only when they are present at the EVPLs.

$$\underset{\mathbf{\Psi}}{\text{Max}}\ pr_n = \sum\nolimits_{i\in I_n}\Big[\frac{(sc^{des}_{n,i} - sc^{arr}_{n,i})BC_{n,i}}{\eta^{ch}}\Pi^{EV} + \sum\nolimits_{t\in H}\Pi^{PL}_t p^{dch}_{n,i,t}\Delta t - \sum\nolimits_{t\in H}\Big[p^{ch}_{n,i,t}\Delta t(\Pi^{PL}_t - \sum\nolimits_{s\in S} D_{n,s}\delta_{n,t,s})\Big] - cost^{deg}_{n,i}\Big]; \forall n \in E \tag{3a}$$

Subject to:

$$cost^{deg}_{n,i} = (BP_{n,i}/EoL)\sum\nolimits_{t\in[t^{arr}_{n,i}, t^{dep}_{n,i}]}\Big[f(p^{EV}_{n,i,t}) - f(\tfrac{(sc^{des}_{n,i} - sc^{arr}_{n,i})BC_{n,i}}{t^{dep}_{n,i} - t^{arr}_{n,i}})\Big]; \forall n \in E, \forall i \in I_n \tag{3b}$$

$$p^{EV}_{n,i,t} = \eta^{ch} p^{ch}_{n,i,t} + p^{dch}_{n,i,t}/\eta^{dch}; \forall n \in E, \forall i \in I_n, \forall t \in H \quad (3c)$$

$$f(p_t) = (\alpha T^2 + \beta T + \gamma) p_t e^{(\zeta T + \kappa) p_t} \Delta t; \forall t \in H \quad (3d)$$

$$sc_{n,i,t+1} = sc_{n,i,t} + \Delta t(\eta^{ch} p^{ch}_{n,i,t} - p^{dch}_{n,i,t}/\eta^{dch})/BC_{n,i} : \lambda^1_{n,i,t}; \quad \forall n \in E, \forall i \in I_n, \forall t \in [t^{arr}_{n,i}, t^{dep}_{n,i}] \quad (3e)$$

$$0 \le p^{ch}_{n,i,t} \le p^{ch,max}_{n,i} : \mu^1_{n,i,t}, \mu^2_{n,i,t}; \forall n \in E, \forall i \in I_n, \forall t \in H \quad (3f)$$

$$0 \le p^{dch}_{n,i,t} \le p^{dch,max}_{n,i} : \mu^3_{n,i,t}, \mu^4_{n,i,t}; \forall n \in E, \forall i \in I_n, \forall t \in H \quad (3g)$$

$$sc^{min}_{n,i} \le sc_{n,i,t} \le sc^{max}_{n,i} : \mu^5_{n,i,t}, \mu^6_{n,i,t}; \forall n \in E, \forall i \in I_n, \forall t \in H \quad (3h)$$

$$sc_{n,i,t} = sc^{arr}_{n,i} : \lambda^2_{n,i,t}; \forall n \in E, \forall i \in I_n, t = t^{arr}_{n,i} \quad (3i)$$

$$sc_{n,i,t} = sc^{des}_{n,i} : \lambda^3_{n,i,t}; \forall n \in E, \forall i \in I_n, t = t^{dep}_{n,i} \quad (3j)$$

$$p^{ch}_{n,i,t} + p^{dch}_{n,i,t} = 0 : \lambda^4_{n,i,t}; \forall n \in E, \forall i \in I_n, \forall t \notin [t^{arr}_{n,i}, t^{dep}_{n,i}] \quad (3k)$$

where $\mathbf{\Psi} = \{p^{ch}_{n,i,t}, p^{dch}_{n,i,t}, sc_{n,i,t}, cost^{deg}_{n,i}, p^{EV}_{n,i,t}\}$ is the set of decision variables in the lower-level problem; and Π^{EV} and Π^{PL}_t are the electricity prices which are sold by the EVPLs to the PEVs and purchased by the EVPLs from the wholesale market, respectively.

4. Uncertainty Modeling

4.1. Uncertainties Related to RES Generation and Demand

In this study, we use predicted conventional demand, EVPL demand, and RES generation to run the day-ahead DN scheduling model. Since forecasting error is inevitable, it is necessary to consider the associated uncertainties. For this purpose, we employ the SSUT method, which is a computationally efficient but accurate approach for considering correlated uncertainties [30, 31].

In this method, we approximate the output vector based on a specific set of sample points from the input. Assuming there are O random variables in the problem, $O+2$ sample points should be selected from the input random variables to form the *sigma point* set. The new set would accurately represent the necessary statistical information of the input [30]. Solving the problem for each of these sigma points, we can approximate the mean and covariance vector of the output.

To better explain the SSUT method, let us consider a problem as $Y = g(Z)$, where g is a linear/nonlinear function, Y is the output vector, and Z is the random input data. The SSUT method is implemented through the following steps:

Step 1: Choose a weight for the zero$^{\text{th}}$ point: $0 \le W_0 \le 1$.

Step 2: Calculate the weight of other sigma points:

$$W_l = (1 - W_0)/(O+1); \ \forall l \in \{0, ..., O+1\} \quad (4)$$

Step 3: Initialize the one-dimensional vector sequence:

$$\chi^1_0 = [0], \ \chi^1_1 = [-\tfrac{1}{2\sqrt{W_1}}], \ \chi^1_2 = [\tfrac{1}{2\sqrt{W_1}}] \quad (5)$$

Step 4: Expand the vector sequence (χ^j_l) for $j = 2, \ldots, O$:

$$\begin{bmatrix} \chi^{j-1}_l \\ 0 \end{bmatrix}_{l=0}, \left[\frac{\chi^{j-1}_l}{\sqrt{j(j+1)W_1}} \right]_{l \in \{1,..,j\}}, \left[\frac{\mathbf{0}_{j-1}}{\sqrt{j(j+1)W_1}} \right]_{l=j+1} \quad (6)$$

where $\mathbf{0}_{j-1}$ is a vector of zeros with a dimension of $j-1$.

Step 5: Calculate the lth sigma point, Z_l:

$$Z_l = \bar{Z} + \sqrt{\Sigma_Z} \chi^O_l; \ \forall l \in \{0, ..., O+1\} \quad (7)$$

where $\sqrt{\Sigma_Z}$ is the square root of the covariance matrix, which can be calculated using numerically efficient and stable methods such as the Cholesky decomposition [32].

Step 6: Calculate corresponding output sigma points by feeding each sigma point into the problem:

$$Y_l = g(Z_l); \ \forall l \in \{0, ..., O+1\} \quad (8)$$

Step 7: Determine the approximated mean and covariance of the output vector, Y:

$$\bar{Y} \approx \sum\nolimits_{l=0}^{O+1} W_l Y_l \quad (9)$$

$$\Sigma_Y \approx \sum\nolimits_{l=0}^{O+1} W_l (Y_l - \bar{Y})(Y_l - \bar{Y})^\intercal \quad (10)$$

In the model proposed in this paper, the input random variables are RES generation, conventional demand, and EVPL demand, while the output is the objective function of the upper-level problem (i.e., the total DSO cost). It is worth noting that the mean and standard deviation of each input random variable are respectively set to its predicted value and forecasting error. Thus, the sample points of the input random variables can be easily determined by implementing the SSUT method using the mentioned procedure (Steps 1 to 5).

These sample points, together with their corresponding weights, can be used to conduct the deterministic day-ahead scheduling problem for the DSO, presented in Subsection 3.1, in a probabilistic manner. To model the uncertainties by considering the set of sample points in the DSO optimization problem, each of the upper-level decision variables (making up $\mathbf{\Phi}$), except the discount binary variables, $\delta_{n,t,s}$, should be calculated for all the sample points (for example, $p^{SS}_{ss,t}$ would be converted to $p^{SS}_{ss,t,l}$ when the uncertainties are considered). Finally, by solving the probabilistic problem and determining the output (the total DSO cost in this problem) for each sample point, we can approximate the expected value of the output, as expressed in (9).

4.2. Uncertainties of PEV Owners' Behavior

As can be seen in (3), the input data includes different characteristics of the PEV users' behavior, including their arrival time, departure time, initial SOC, and desired SOC. Using the parking lot traffic data, the behavior of the PEV owners can be estimated. However, if sufficient historical data for PEV trips is not available, the uncertainties associated with PEV owners' behavior can be modeled by using the statistical model of the PEV data to generate scenarios for their arrival time, departure time, initial SOC, and desired SOC.

To this end, we employ truncated Gaussian probability distribution functions (PDFs) to generate scenarios for arrival and departure times as well as initial SOC level of PEVs [19]. Also, the scenarios for the desired SOC levels of PEVs can be generated by using either a uniform (for workplace parking lots) or a truncated exponential PDF (for commercial parking lots). Next, we estimate the mean and the standard deviation of the Gaussian and exponential PDFs as well as the range of all PDFs of users' characteristics by using historical data or educated guess by the experts. Finally, using the derived PDF for each PEV user's characteristics (arrival time, departure time, initial SOC, and desired SOC), we generate the scenarios for the respective characteristics of PEVs of each parking lot. Interested readers are referred to [31] for more details.

5. Solution Method

5.1. Piecewise Linearization of Nonlinear Functions

As mentioned before, we aim to develop a MILP model so that convergence to the global optimum can be guaranteed. However, equations (1a) and (3d) are nonlinear, even though they are convex. We can readily linearize such functions with the following piecewise linearization method without needing binary variables, ensuring that the problem will be linear.

Suppose $F(x)$ is a convex function over $0 < x < \bar{x}$, but it is not linear with respect to x, e.g., xe^x and x^2. To linearize $F(x)$, we can approximate it with a piecewise linear function, $G(x)$. For this purpose, (11)–(13) can be added to the problem to replace $F(x)$, while (14) and (15) are used to determine the associated parameters. It is also worth noting that, for a definite number of segments ($||PC||$), the exact size of the segments (A_{pc}) can be chosen so as to minimize the approximation error ($\int_0^{\bar{x}} |F(x) - G(x)|dx$).

$$G = \sum\nolimits_{pc \in PC} K_{pc} u_{pc} \tag{11}$$

$$x = \sum\nolimits_{pc \in PC} u_{pc} \tag{12}$$

$$0 \leq u_{pc} \leq A_{pc}; \forall pc \in PC \tag{13}$$

$$\sum\nolimits_{pc \in PC} A_{pc} = \bar{x} \tag{14}$$

$$K_{pc} = \frac{f(\sum_{q=1}^{pc} A_q) - f(\sum_{q=1}^{pc-1} A_q)}{A_{pc}}; \forall pc \in PC \tag{15}$$

Based on the above method, we linearized the first term in equation (1a), $cost_{los}$, and $f(p_t)$ in (3d). As an illustration, $f(p_t)$ has been linearized through (16)–(18).

$$f(p_t) = \sum\nolimits_{pc \in PC} K_{pc}^{EV} p_{t,pc}^{pw}; \forall t \in H \tag{16}$$

$$p_t = \sum\nolimits_{pc \in PC} p_{t,pc}^{pw}; \forall t \in H \tag{17}$$

$$0 \leq p_{t,pc}^{pw} \leq \frac{p_t^{max}}{||PC||}; \forall t \in H, \forall pc \in PC \tag{18}$$

5.2. Casting the Bi-Level Problem into a Single-Level Problem

As mentioned in Section 2, we should either use the KKT optimality conditions or the strong duality theorem to find the global optimal solutions to the proposed bi-level problem. This way, the lower-level problems will be represented by a set of constraints in the upper-level problem. As the lower-level problems are linear programs (LPs), strong duality holds if the primal and dual problems are feasible [33]. Thus, we can readily cast the bi-level problem as a single-level MILP model with the following structure:

$$\begin{cases} \textit{Minimize} \;\; \text{Total cost of the DSO, (1a)} \\ \textit{Subject to}: \\ \quad \text{Upper-level problem constraints, linearized (1b)–(1l)} \\ \quad \text{Lower-level problem constraints, (3b)–(3k)} \\ \quad \text{Constraints of dual lower-level problems} \\ \quad \text{Optimal duality gap of lower-level problems} = 0 \end{cases}$$

To achieve a single-level MILP problem using the KKT optimality conditions, Fortuny-Amat and McCarl method should be used for linearizing the nonlinear KKT conditions [34]. The resulting binary linear constraints of the lower-level problems can then be added to the upper-level problem, forming a single-level MILP problem, as represented in the following:

$$\begin{cases} \textit{Minimize} \;\; \text{Total cost of the DSO, (1a)} \\ \textit{Subject to}: \\ \quad \text{Upper-level problem constraints, linearized (1b)–(1l)} \\ \quad \text{Lower-level problem constraints, (3b)–(3k)} \\ \quad \text{Binary-linear KKT conditions of lower-level problems} \end{cases}$$

The mathematical formulations of the KKT conditions and the dual of lower-level problems are available in detail in Appendix A.

5.3. Linearizing the AC OPF

As noted in Section 3, we linearize the AC OPF equations, (1g)–(1l), based on the two-stage procedure proposed in [35]. To this end, at the first stage, the problem is solved considering nominal voltages equal to one per unit (i.e., a cold start) by neglecting losses in the OPF equations. The solution to the first stage (nodal voltages and active/reactive power flow of lines) is then utilized to initialize the second stage, and the problem is solved one more time to obtain the optimal solution.

To decrease the computational burden in this paper, we

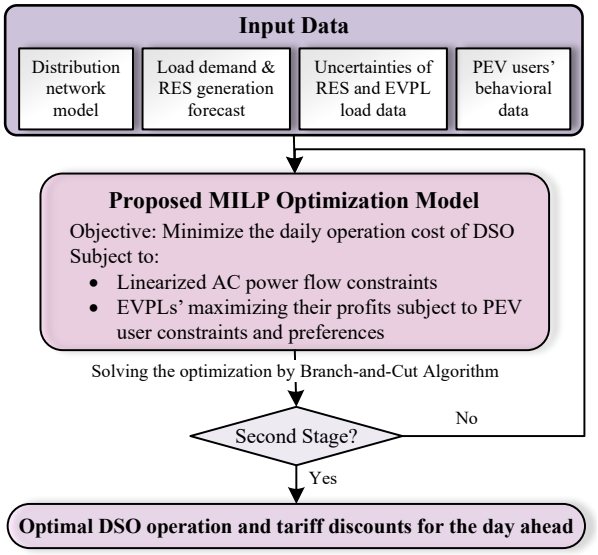

Figure 2: Flowchart of the overall workflow for using the model.

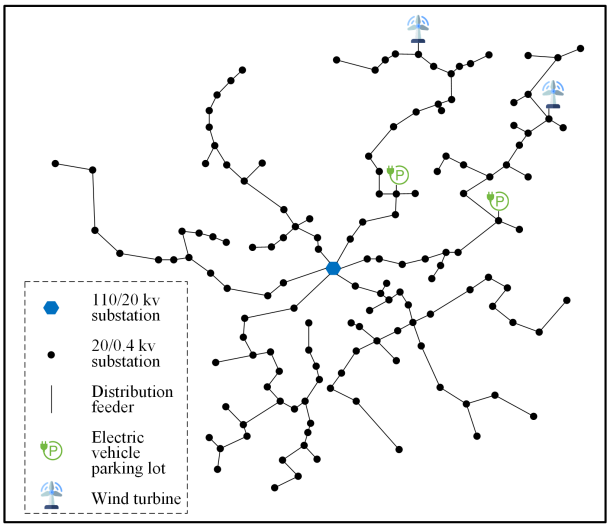

Figure 3: Single-line diagram of the test DN.

solve a slightly different problem at the first stage without considering DSO's discounts so that the optimization problem can be solved faster. The solution to the first stage is then used to initialize the second stage. It is worth noting that if we employ the strong duality theorem to convert the bi-level problem into an equivalent single-level one, the equations related to the lower-level problems will be linear. Thus, in the proposed approach, the optimal solutions are determined through solving an LP (at the first stage) and a MILP problem (at the second stage) rather than two MILP problems.

Table 2: Statistical data of the truncated Gaussian PDFs

	Characteristic	Mean	STD	Min	Max
EVPL 1	Arrival time	8	2	6	11
	Departure time	16	2	12	20
	Initial SOC	0.5	0.3	0.2	0.8
EVPL 2	Arrival time	13	2	9	17
	Departure time	17	2	14	20
	Initial SOC	0.5	0.3	0.2	0.8

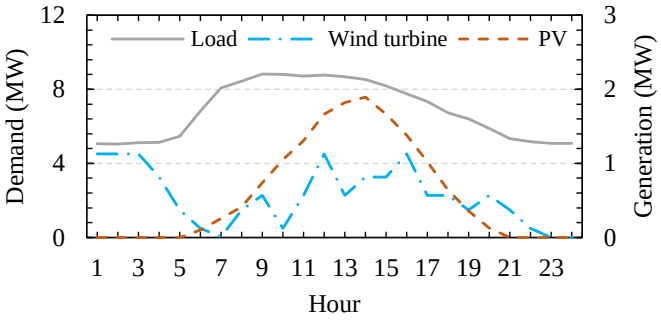

Figure 4: The RES generation and the load demand on the typical summer day.

6. Simulation Studies

6.1. Test System Description

The flowchart in Fig. 2 shows the overall workflow to find the global optimal solution using the proposed model. To investigate the effectiveness and applicability of the model, it is implemented on a typical Finnish DN [36], comprising 144 load nodes and a substation, which is depicted in Fig. 3. The data for conventional load profiles and PV generation are obtained from [37] and [38], respectively. Also, wind speed data are collected from [39], while the power curve for the wind turbine generator is based on a 900 kW E44 Enercon wind turbine [40]. The day-ahead energy and regulation prices are gathered from [41]. Also, the forecasting errors of RES generation, conventional demand, and EVPL demand are set to 20%, 5%, and 10%, respectively.

In the simulation studies, as shown in Fig. 3, two EVPLs are considered in the area connected to the DN, and the number of PEVs arriving in each parking lot is 300. Although the numbers of PEVs parked in the EVPLs are the same, the first one is located near office buildings while the second one is placed near a shopping center. As noted in Section 4, we have employed truncated Gaussian PDFs to generate scenarios for arrival and departure times, and the initial SOC level of PEVs. Table 2 shows the statistical data of the PDFs used for generating the scenarios of the mentioned PEV characteristics. Also, the scenarios for the desired SOC levels of PEVs are generated by using a uniform PDF from 80% to 100% for the first EVPL (i.e., the workplace parking lot) and a truncated exponential

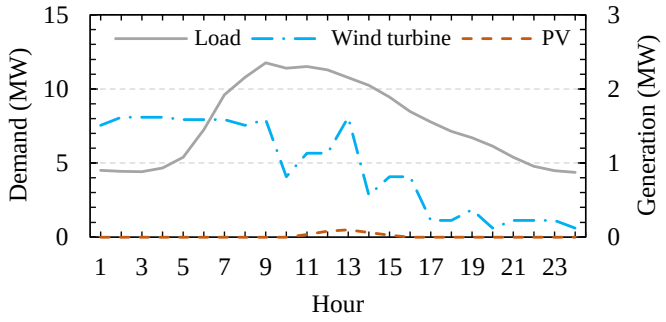

Figure 5: The RES generation and the load demand on the typical winter day.

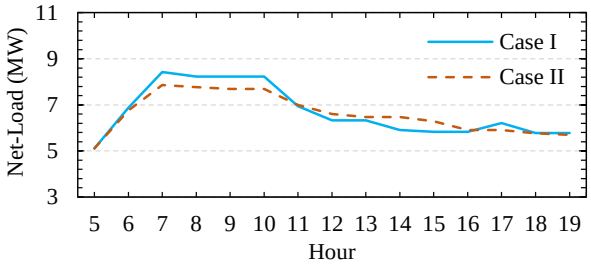

Figure 6: The DN net-load on the summer day.

PDF from the PEV initial SOC to 100% with the lambda coefficient set to three for EVPL 2 (i.e., the commercial parking lot).

It is worth mentioning that the net-load ramping up/down penalty on each day is equal to the average of the regulation up/down prices in seven previous days. Also, the simulations are performed for a typical day in summer and winter. Figs. 4 and 5 represent the generation of wind turbines and photovoltaic (PV) systems as well as the load demand in the test DN on the typical summer and winter days, respectively. Lastly, it is assumed that the DSO considers two discount steps for EVPLs, 5% and 15% of the EVPL electricity prices. Other data for the simulation study can be found at [42].

We implemented the proposed MILP optimization model in GAMS 24.8 and solved by using IBM CPLEX 12.8 with a Branch-and-Bound algorithm. The simulation studies were carried out on a Fujitsu CELSIUS W530 PC with an Intel Xeon E3-1230 3.20 GHz processor and 32 GB of RAM.

6.2. Analyzing Flexibility Provision by EVPLs

To investigate the effectiveness of the proposed approach in decreasing the flexibility requirement of the DSO, we have studied two cases. In **Case I**, no discount on the network tariff is offered to EVPLs, while, in **Case II**, the EVPLs provide flexibility by receiving discounts at different times of the day. The simulation studies have been carried out for both cases on the typical summer and winter days. Two flexibility indices are used to measure flexibility improvement, PAR and peak-off-peak (PoP) difference of the DN net-load.

Both strong duality-based and KKT-based approaches were used to recast the model as a single-level MILP problem. However, as numerous binary variables were introduced to linearize the complementary constraints in the KKT-based approach, the solver could not reach the optimality gap of 1% in less than 20 hours in Case II. Thus, we used the strong duality-based method as a computationally efficient option to obtain the optimal solutions.

The simulation results obtained for the two cases are given in Table 3. The PoP difference and PAR are reduced by 13% and 6%, respectively, on the typical summer day and 15% and 24%, respectively, on the typical winter day in Case II in comparison with Case I, which indicates the effectiveness of the method in providing flexibility by the EVPLs. Moreover, the discounts offered by the DSO led to a reduction in the total cost of the DSO, while the total profits of the two EVPLs increased compared to Case I. To be more specific, by the network tariff discounts in some hours, the DSO financially motivates the EVPL operators to manage PEVs charging such that the DN ramping rates are decreased. This, in turn, leads to less flexibility-oriented cost and RES generation curtailment. It demonstrates that, under the new regulations, implementing the proposed method not only enables the DSO to utilize the EVPLs' flexibility but also offers financial benefits to both the DSO and the EVPLs. The proposed incentive-based framework can also be leveraged to encourage EVPL operators to provide other necessary services to the DN.

The DN net-loads on the summer and winter days for the scenario with perfect prediction are shown in Figs. 6 and 7, respectively. It can be seen in the figures that the net-load demand is shifted in time to smooth the net-load profile in Case II. Also, the net-load ramp rates have reduced in Case II in comparison with Case I. As an illustration, the ramp rates of the DN net-load on the summer day for both cases are shown in Fig. 8. According to the figure, the steep ramps in many hours of the day are alleviated by implementing the proposed model. In addition, it can be seen that the ramp rates are decreased more at midday compared to the rest of the day. This is because the number of PEVs parked in the EVPLs is at its maximum at midday, so there are more batteries to provide flexibility at this time of the day. Nevertheless, it seems that the proposed method was more effective on the winter day, as can be inferred from Table 3 by comparing the PAR and PoP reduction on the summer and winter days. This is mainly because the ramp rates on the winter day are higher than those on the summer day, which can lead to a higher contribution from the EVPL operators in providing flexibility.

6.3. Evaluating the Proposed Two-Stage Method Accuracy

As noted in Section 5, we decided to eliminate the DSO's discounts at the first stage of the linearized OPF equations, proposed in [35], to reduce the computation

Table 3: Simulation results for Cases I and II

	Summer day		Winter day	
	Case I	Case II	Case I	Case II
PAR	1.43	1.34	1.76	1.34
PoP difference (MW)	4.50	3.92	9.25	7.87
$cost_{los}$ (€)	141.2	139.2	185.8	182.9
$cost_{cur}$ (€)	92.2	17.1	36.3	2.8
$cost_{flex}$ (€)	499.9	395.5	828.3	689.2
$cost_{dis}$ (€)	–	65.4	–	57.0
Total DSO cost (€)	733.3	617.2	1050.3	931.9
EVPL 1 profit (€)	136.6	167.7	183.8	207.3
EVPL 2 profit (€)	40.7	45.0	57.6	57.6
Simulation time (h)	0.3	9.7	0.4	0.9

Table 4: Results for our proposed and the original two-stage methods

	Summer day		Winter day	
OPF Approach	Original	Proposed	Original	Proposed
$cost_{los}$ (€)	139.2	139.2	182.6	182.9
$cost_{cur}$ (€)	17.2	17.1	3.9	2.8
$cost_{flex}$ (€)	395.1	395.5	689.0	689.2
$cost_{dis}$ (€)	65.4	65.4	57.2	57.0
Total DSO cost (€)	616.8	617.2	932.6	931.9
EVPL 1 profit (€)	167.7	167.7	207.2	207.3
EVPL 2 profit (€)	45.0	45.0	57.8	57.6
Simulation time (h)	17.5	9.7	1.5	0.9

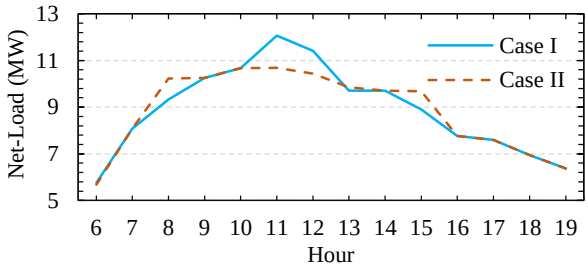

Figure 7: The DN net-load on the winter day.

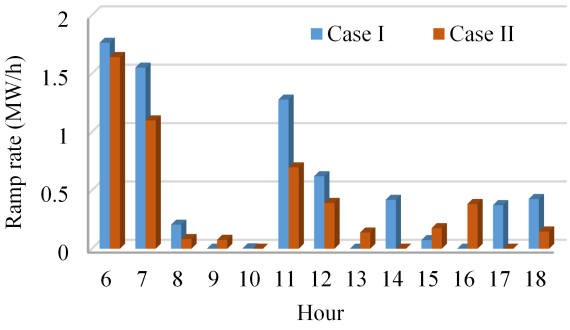

Figure 8: The ramp rates of the DN net-load on the summer day.

time. We then considered them at the second stage. Since the solution to the first stage problem is used to initialize the second stage, it is essential to evaluate the impact of this modification on the accuracy of the optimal solutions. For this purpose, the results of our proposed approach and the original method in [35] are compared for the summer and winter days in Table 4.

According to the table, the differences between the financial terms in the original and the proposed methods are negligible on both days, particularly in the objective functions of the upper- and lower-level problems, i.e., total DSO cost and EVPLs' profit, respectively. However, more than 40% reduction in simulation time has been achieved for the proposed method in comparison with the original one.

6.4. Investigating the Performance of the PEV Battery Degradation Model

To analyze the accuracy of the proposed battery degradation model, we compare the cost of battery degradation caused by EVPLs' flexibility provision in the proposed model with that obtained by using the models in the existing literature on the subject of our study [18, 19, 21, 22] and the model proposed in [29], which is derived based on practical experiments. The costs of battery degradation on a typical winter day caused by EVPLs' flexibility provision are 10.4€, 5.1€, and 12.1€ for the proposed model; the ones in [13, 18, 19, 21, 22]; and [29], respectively. If we

take the model developed in [29] as the benchmark, our linear model shows a much higher accuracy compared to those in [13, 18, 19, 21, 22].

7. Conclusion

In this paper, we developed a day-ahead scheduling model for DSOs, in which the EVPLs connected to the DN were considered for flexibility provision. Although the main goal of EVPL operators is to maximize their profit while meeting the PEV owners' requirements, the DSO can provide incentives, e.g., discounts on the network tariff, to exploit their inherent flexibility throughout a day. To model the behavior of the DSO and the EVPL operators, we developed a mathematical formulation based on bi-level programming, which was converted to an equivalent single-level problem using the strong duality theorem. Additionally, we used more accurate approaches to linearize AC OPF equations and to model PEV battery degradation, compared to the existing literature in the field. The developed model was implemented on a 145-bus test DN with high penetration of RESs. The simulation results showed that, under regulatory policies, using the proposed model not only can financially benefit the DSO and the EVPL operators but also can smooth the network net-load (i.e., decrease the ramp rates). In the results, the financial benefits of the proposed method were reflected by the reduction of the DSO cost and the increase in the profits of EVPLs, while the effectiveness in utilizing PEVs' flexibility was demonstrated by the improvements of two flexibility indices, PoP difference and PAR. Moreover, the benefits of the methods used for the linearized AC OPF equations and the PEV battery degradation model were validated in the numerical results. Once the financial benefit of the proposed model for the EVPLs' operators has been demonstrated, they can be encouraged to provide other kinds of services for the DSO. The future work considers extending the current model for including the provision of other services like energy arbitrage and choosing among different opportunities of providing services.

Appendix A. Casting the Bi-Level Problem into Single-Level Problem

As mentioned in the paper, to cast the model into a MILP form, we not only linearized nonlinear terms but also converted the bi-level problem into a single-level one. To this end, we tried both the strong duality theorem and KKT conditions to consider the lower-level problems, described in Subsection 3.2, as a set of constraints in the upper-level. For this purpose, the Lagrangian function of each lower-level problem is determined according to (A.1). Based on the Lagrangian function, mathematical models of both methods are represented in the following.

Appendix A.1. Using Strong Duality Theorem

To convert the bi-level problem into a single-level one, we can use the strong duality theorem, replacing each lower-level problem with a set of constraints. In each of these sets, we should set the optimal duality gap of the lower-level problem equal to zero (i.e., the objective functions of dual and primal problems should be equal) while considering the constraints of primal and dual lower-level problems. It is evident that strong duality holds if the primal and dual problems are feasible [33].

The primal of lower-level problems is described in Subsection 3.2. Here, we write the dual of the lower-level problems by using the Lagrangian function (A.1). The objective function of the dual problem is represented in (A.2), while (A.3)–(A.11) denote its constraints. Also, (A.12)–(A.14) specify the feasible regions of dual variables.

$$\begin{aligned}\text{Min}\ \ OF_n^{Dual} = \sum_{i\in I_n}\Big[\sum_{t\in H}[p_{n,i,t}^{ch,max}\mu_{n,i,t}^{2} + p_{n,i,t}^{dch,max}\mu_{n,i,t}^{4} \\ - sc_{n,i}^{min}\mu_{n,i,t}^{5} + sc_{n,i}^{max}\mu_{n,i,t}^{6}] + sc_{n,i}^{arr}\lambda_{n,i,t}^{2}|_{t=t_{n,i}^{arr}} \\ + sc_{n,i}^{des}\lambda_{n,i,t}^{3}|_{t=t_{n,i}^{dep}} + \sum_{t\in H}\sum_{pc\in PC} A_{n,i,pc}^{EV}\mu_{n,i,t,pc}^{EV,2}\Big]; \forall n\in E\end{aligned} \tag{A.2}$$

$$\begin{aligned}\frac{\partial L}{\partial p_{n,i,t}^{ch}} = -\Delta t(\Pi_t^{PL} - \sum_{s\in S} D_{n,s}\delta_{n,t,s}) + \mu_{n,i,t}^{1} - \mu_{n,i,t}^{2} \\ + \Delta t\eta^{ch}\lambda_{n,i,t}^{1}/BC_{n,i,k} + \eta^{ch}\lambda_{n,i,t}^{EV,1} = 0; \\ \forall n\in E, \forall i\in I_n, \forall t\in[t_{n,i}^{arr}, t_{n,i}^{dep}]\end{aligned} \tag{A.3}$$

$$\begin{aligned}\frac{\partial L}{\partial p_{n,i,t}^{ch}} = -\Delta t(\Pi_t^{PL} - \sum_{s\in S} D_{n,s}\delta_{n,t,s}) + \mu_{n,i,t}^{1} - \mu_{n,i,t}^{2} + \lambda_{n,i,t}^{4} \\ + \eta^{ch}\lambda_{n,i,t}^{EV,1} = 0; \forall n\in E, \forall i\in I_n, \forall t\notin[t_{n,i}^{arr}, t_{n,i}^{dep}]\end{aligned} \tag{A.4}$$

$$\begin{aligned}\frac{\partial L}{\partial p_{n,i,t}^{dch}} = \Delta t\Pi_t^{PL} + \mu_{n,i,t}^{3} - \mu_{n,i,t}^{4} - \Delta t\lambda_{n,i,t}^{1}/(\eta^{dch}BC_{n,i,k}) \\ + \lambda_{n,i,t}^{EV,1}/\eta^{dch} = 0; \forall n\in E, \forall i\in I_n, \forall t\in[t_{n,i}^{arr}, t_{n,i}^{dep}]\end{aligned} \tag{A.5}$$

$$\begin{aligned}\frac{\partial L}{\partial p_{n,i,t}^{dch}} = \Delta t\Pi_t^{PL} + \mu_{n,i,t}^{3} - \mu_{n,i,t}^{4} + \lambda_{n,i,t}^{4} + \lambda_{n,i,t}^{EV,1}/\eta^{dch} = 0; \\ \forall n\in E, \forall i\in I_n, \forall t\notin[t_{n,i}^{arr}, t_{n,i}^{dep}]\end{aligned} \tag{A.6}$$

$$\begin{aligned}\frac{\partial L}{\partial sc_{n,i,t}} = \lambda_{n,i,t-1}^{1} - \lambda_{n,i,t}^{1} + \mu_{n,i,t}^{5} - \mu_{n,i,t}^{6} = 0; \forall n\in E, \\ \forall i\in I_n, \forall t\in[t_{n,i}^{arr}, t_{n,i}^{dep}], t\neq t_{n,i}^{arr}, t\neq t_{n,i}^{dep}\end{aligned} \tag{A.7}$$

$$\begin{aligned}\frac{\partial L}{\partial sc_{n,i,t}} = \lambda_{n,i,t-1}^{1} - \lambda_{n,i,t}^{1} + \lambda_{n,i,t}^{2} + \mu_{n,i,t}^{5} - \mu_{n,i,t}^{6} = 0; \\ \forall n\in E, \forall i\in I_n, t = t_{n,i}^{arr}\end{aligned} \tag{A.8}$$

$$\mathcal{L}(p^{ch}_{n,i,t}, p^{dch}_{n,i,t}, sc_{n,i,t}, p^{EV,pw}_{n,i,t,pc}, \mu, \lambda) = \sum_{i\in I_n}\Bigg[\sum_{t\in H}\Bigg[\Big[\Pi^{PL}_t p^{dch}_{n,i,t}\Delta t - \big[p^{ch}_{n,i,t}\Delta t(\Pi^{PL}_t - \sum_{s\in S} D_{n,s}\delta_{n,t,s})\Big]$$
$$- \sum_{pc\in PC} K^{EV}_{pc} BP_{n,i} p^{EV,PW}_{n,i,t,pc}/EoL\Big] + \Big[p^{ch}_{n,i,t}\Big]\mu^1_{n,i,t} + \Big[p^{ch,max}_{n,i,t} - p^{ch}_{n,i,t}\Big]\mu^2_{n,i,t} + \Big[p^{dch}_{n,i,t}\Big]\mu^3_{n,i,t} + \Big[p^{dch,max}_{n,i,t} - p^{dch}_{n,i,t}\Big]\mu^4_{n,i,t}$$
$$+ \Big[sc_{n,i,t} - sc^{min}_{n,i}\Big]\mu^5_{n,i,t} + \Big[sc^{max}_{n,i} - sc_{n,i,t}\Big]\mu^6_{n,i,t} + \Big[p^{EV}_{n,i,t} - \sum_{pc\in PC} p^{EV,pw}_{n,i,t,pc}\Big]\lambda^{EV,1}_{n,i,t} + \sum_{pc\in PC}\Big[p^{EV,pw}_{n,i,t,pc}\mu^{EV,1}_{n,i,t,pc}$$
$$+ (A^{EV}_{n,i,pc} - p^{EV,pw}_{n,i,t,pc})\mu^{EV,2}_{n,i,t,pc}\Big]\Bigg] + \sum_{t\in[t^{arr}_{n,i}, t^{dep}_{n,u}]}\Bigg[\Big[sc_{n,i,t+1} - sc_{n,i,t} + \Delta t(\eta^{ch} p^{ch}_{n,i,t} - p^{dch}_{n,i,t}/\eta^{dch})/BC_{n,i,k}\Big]\lambda^1_{n,i,t}\Bigg]$$
$$+ \Bigg[\Big[sc_{n,i,t} - sc^{arr}_{n,i}\Big]\lambda^2_{n,i,t}\Bigg]_{t=t^{arr}_{n,i}} + \Bigg[\Big[sc_{n,i,t} - sc^{des}_{n,i}\Big]\lambda^3_{n,i,t}\Bigg]_{t=t^{dep}_{n,i}} + \sum_{t\notin[t^{arr}_{n,i}, t^{dep}_{n,u}]}\Bigg[\Big[p^{ch}_{n,i,t} + p^{dch}_{n,i,t}\Big]\lambda^4_{n,i,t}\Bigg]\Bigg]; \forall n\in E \tag{A.1}$$

$$\frac{\partial L}{\partial sc_{n,i,t}} = \lambda^1_{n,i,t-1} - \lambda^1_{n,i,t} + \lambda^3_{n,i,t} + \mu^5_{n,i,t} - \mu^6_{n,i,t} = 0;$$
$$\forall n\in E, \forall i\in I_n, t = t^{dep}_{n,i} \tag{A.9}$$

$$\frac{\partial L}{\partial sc_{n,i,t}} = \mu^5_{n,i,t} - \mu^6_{n,i,t} = 0;$$
$$\forall n\in E, \forall i\in I_n, \forall t\notin [t^{arr}_{n,i}, t^{dep}_{n,i}] \tag{A.10}$$

$$\frac{\partial L}{\partial p^{EV,pw}_{n,i,t,pc}} = -K^{EV}_{pc} BP_{n,i}/EoL - \lambda^{EV,1}_{n,i,t} + \mu^{EV,1}_{n,i,t,pc} - \mu^{EV,2}_{n,i,t,pc}$$
$$= 0; \forall n\in E, \forall i\in I_n, \forall t\in H, \forall pc\in PC \tag{A.11}$$

$$\mu^1_{n,i,t}, \mu^2_{n,i,t}, \mu^3_{n,i,t}, \mu^4_{n,i,t}, \mu^5_{n,i,t}, \mu^6_{n,i,t} \in \mathbb{R}^+;$$
$$\forall n\in E, \forall i\in I_n, \forall t\in H \tag{A.12}$$

$$\mu^{EV,1}_{n,i,t,pc}, \mu^{EV,2}_{n,i,t,pc} \in \mathbb{R}^+;$$
$$\forall n\in E, \forall i\in I_n, \forall t\in H, \forall pc\in PC \tag{A.13}$$

$$\lambda^1_{n,i,t}, \lambda^2_{n,i,t}, \lambda^3_{n,i,t}, \lambda^4_{n,i,t}, \lambda^{EV,1}_{n,i,t} \in \mathbb{R};$$
$$\forall n\in E, \forall i\in I_n, \forall t\in H \tag{A.14}$$

Appendix A.2. Using KKT Conditions

As mentioned previously, we can also convert the bi-level problem into a single-level one by using the KKT conditions of lower-level problems. To ensure that each lower-level problem is optimized, its KKT conditions should be satisfied in the upper-level problem.

Using the Lagrangian function of the lower-level problems (A.1), the KKT conditions are imposed through (A.3)–(A.11), (A.15)–(A.22), and (A.12)–(A.14), which ensure stationarity, complementary slackness, and dual feasibility of the conditions, respectively. Thus, the bi-level problem will be cast as single-level one by considering the KKT conditions of each lower-level problem together with its primal constraints in the upper-level problem [28].

$$p^{ch}_{n,i,t}\cdot\mu^1_{n,i,t} = 0; \forall n\in E, \forall i\in I_n, \forall t\in H \tag{A.15}$$

$$(p^{ch,max}_{n,i,t} - p^{ch}_{n,i,t})\cdot\mu^2_{n,i,t} = 0; \forall n\in E, \forall i\in I_n, \forall t\in H \tag{A.16}$$

$$p^{dch}_{n,i,t}\cdot\mu^3_{n,i,t} = 0; \forall n\in E, \forall i\in I_n, \forall t\in H \tag{A.17}$$

$$(p^{dch,max}_{n,i,t} - p^{dch}_{n,i,t})\cdot\mu^4_{n,i,t} = 0; \forall n\in E, \forall i\in I_n, \forall t\in H \tag{A.18}$$

$$(sc_{n,i,t} - sc^{min}_{n,i})\cdot\mu^5_{n,i,t} = 0; \forall n\in E, \forall i\in I_n, \forall t\in H \tag{A.19}$$

$$(sc^{max}_{n,i} - sc_{n,i,t})\cdot\mu^6_{n,i,t} = 0; \forall n\in E, \forall i\in I_n, \forall t\in H \tag{A.20}$$

$$p^{EV,pw}_{n,i,t,pc}\cdot\mu^{EV,1}_{n,i,t,pc} = 0; \forall n\in E, \forall i\in I_n, \forall t\in H, \forall pc\in PC \tag{A.21}$$

$$(A^{EV}_{n,i,pc} - p^{EV,pw}_{n,i,t,pc})\cdot\mu^{EV,2}_{n,i,t,pc} = 0;$$
$$\forall n\in E, \forall i\in I_n, \forall t\in H, \forall pc\in PC \tag{A.22}$$

As the equations of complementary slackness conditions are nonlinear, Fortuny-Amat and McCarl method [34] should be used to replace (A.15)–(A.22) with binary linear equations for imposing KKT conditions. As a result, the obtained MILP problem can be readily solved by off-the-shelf solvers. To linearize non-linear complementary constraint, which has a general form of $a\cdot b = 0$ for $a, b \geq 0$, each nonlinear equation should be replaced with the following equations:

$$0 \leq a \leq x \times M \tag{A.23}$$

$$0 \leq b \leq (1-x) \times M \tag{A.24}$$

where M is a sufficiently large constant and x is a binary variable.

References

[1] Global ev outlook 2020, Tech. rep., IEA (2020).
URL https://webstore.iea.org/global-ev-outlook-2020

[2] Global renewables outlook: Energy transformation 2050, Tech. rep., IRENA (2020).
URL https://www.irena.org/publications/2020/Apr/Global-Renewables-Outlook-2020

[3] H. Mountford, D. Waskow, L. Gonzalez, C. Gajjar, N. Cogswell, M. Holt, T. Fransen, M. Bergen, R. Gerholdt, Cop26: Key outcomes from the un climate talks in glasgow (2021).

[4] Electric power system flexibility: Challenges and opportunities, Tech. rep., EPRI (2016).
URL https://www.naseo.org/Data/Sites/1/flexibility-white-paper.pdf

[5] A. Majzoobi, A. Khodaei, Application of microgrids in supporting distribution grid flexibility, IEEE Trans. Power Syst 32 (5) (2017) 3660–3669.

[6] H. K. Nguyen, A. Khodaei, Z. Han, Incentive mechanism design for integrated microgrids in peak ramp minimization problem, IEEE Trans. Smart Grid 9 (6) (2018) 5774–5785.

[7] J. Cochran, M. Miller, O. Zinaman, M. Milligan, D. Arent, B. Palmintier, M. O'Malley, S. Mueller, E. Lannoye, A. Tuohy, et al., Flexibility in 21st century power systems, Tech. rep., National Renewable Energy Lab.(NREL), Golden, CO (United States) (2014).

[8] E. Lannoye, D. Flynn, M. O'Malley, Evaluation of power system flexibility, IEEE Trans. Power Syst 27 (2) (2012) 922–931.

[9] White paper 3 facilitating flexibility, Tech. rep., European Energy Regulators (ACER-CEER) (May 2017).

[10] Incentives schemes for regulating dsos, including for innovation (January 2017).

[11] S. Karimi-Arpanahi, M. Jooshaki, M. Moeini-Aghtaie, A. Abbaspour, M. Fotuhi-Firuzabad, Incorporating flexibility requirements into distribution system expansion planning studies based on regulatory policies, Int. J. Electr. Power Energy Syst 118 (2020) 105769.

[12] N. I. Nimalsiri, E. L. Ratnam, C. P. Mediwaththe, D. B. Smith, S. K. Halgamuge, Coordinated charging and discharging control of electric vehicles to manage supply voltages in distribution networks: Assessing the customer benefit, Appl. Energy 291 (2021) 116857.

[13] X. Lu, K. W. Chan, S. Xia, M. Shahidehpour, W. H. Ng, An operation model for distribution companies using the flexibility of electric vehicle aggregators, IEEE Trans. Smart Grid 12 (2) (2021) 1507–1518.

[14] C. Wei, J. Xu, S. Liao, Y. Sun, Aggregation and scheduling models for electric vehicles in distribution networks considering power fluctuations and load rebound, IEEE Trans. Sustain. Energy 11 (4) (2020) 2755–2764.

[15] Z. Liu, et al., Distribution locational marginal pricing for optimal electric vehicle charging through chance constrained mixed-integer programming, IEEE Trans. Smart Grid 9 (2) (2018) 644–654.

[16] S. Huang, Q. Wu, Dynamic subsidy method for congestion management in distribution networks, IEEE Trans. Smart Grid 9 (3) (2018) 2140–2151.

[17] E. R. Muñoz, F. Jabbari, A decentralized, non-iterative smart protocol for workplace charging of battery electric vehicles, Appl. Energy 272 (2020) 115187.

[18] N. Neyestani, M. Y. Damavandi, M. Shafie-Khah, A. G. Bakirtzis, J. P. Catalao, Plug-in electric vehicles parking lot equilibria with energy and reserve markets, IEEE Trans. Power Syst 32 (3) (2017) 2001–2016.

[19] M. Shafie-Khah, P. Siano, D. Z. Fitiwi, N. Mahmoudi, J. P. Catalao, An innovative two-level model for electric vehicle parking lots in distribution systems with renewable energy, IEEE Trans. Smart Grid 9 (2) (2018) 1506–1520.

[20] S. Aghajani, M. Kalantar, Operational scheduling of electric vehicles parking lot integrated with renewable generation based on bilevel programming approach, Energy 139 (2017) 422–432.

[21] S. M. B. Sadati, J. Moshtagh, M. Shafie-khah, A. Rastgou, J. P. Catalão, Operational scheduling of a smart distribution system considering electric vehicles parking lot: A bi-level approach, Int. J. Electr. Power Energy Syst 105 (2019) 159–178.

[22] R. Mehta, D. Srinivasan, A. M. Khambadkone, J. Yang, A. Trivedi, Smart charging strategies for optimal integration of plug-in electric vehicles within existing distribution system infrastructure, IEEE Trans. Smart Grid 9 (1) (2018) 299–312.

[23] S. A. Talberg, N. J. Saari, R. A. Eubanks, Report on the study of performance-based regulation, Tech. rep., Michigan Public Service Commission, Department of Licensing and Regulatory Affairs (April 2018).

[24] A. Ter-Martirosyan, J. Kwoka, Incentive regulation, service quality, and standards in us electricity distribution, Journal of Regulatory Economics 38 (3) (2010) 258–273.

[25] S. Viljainen, Regulation design in the electricity distributuion sector (2005).

[26] Electricity distribution network tariffs, ceer guidelines of good practice, Tech. rep., Council of European Energy Regulators (CEER) (Jan 2017).

[27] J. M. Arroyo, Bilevel programming applied to power system vulnerability analysis under multiple contingencies, IET Gener. Transm. Distrib 4 (2) (2010) 178–190.

[28] E. Castillo, A. J. Conejo, P. Pedregal, R. Garcia, N. Alguacil, Building and solving mathematical programming models in engineering and science, John Wiley & Sons, New York, NY, USA, 2011.

[29] D. Wang, J. Coignard, T. Zeng, C. Zhang, S. Saxena, Quantifying electric vehicle battery degradation from driving vs. vehicle-to-grid services, J. Power Sources 332 (2016) 193–203.

[30] S. J. Julier, The spherical simplex unscented transformation, in: Proc. of Amer. Control Conf, 2003, pp. 2430–2434.

[31] S. Karimi-Arpanahi, M. Jooshaki, M. Moein-Aghtaie, M. Fotuhi-Firuzabad, M. Lehtonen, Considering forecasting errors in flexibility-oriented distribution network expansion planning using the spherical simplex unscented transformation, IET Gener. Transm. Distrib 14 (24) (2020) 5970–5983.

[32] S. J. Julier, J. K. Uhlmann, Unscented filtering and nonlinear estimation, Proceedings of the IEEE 92 (3) (2004) 401–422.

[33] S. Boyd, L. Vandenberghe, Convex Optimization, Cambridge Univ. Press, New York, NY, USA, 2004.

[34] J. Fortuny-Amat, B. McCarl, A representation and economic interpretation of a two-level programming problem, J. Oper. Res. Soc 32 (9) (1981) 783–792.

[35] J. F. Franco, L. F. Ochoa, R. Romero, Ac opf for smart distribution networks: An efficient and robust quadratic approach, IEEE Trans. Smart Grid 9 (5) (2018) 4613–4623.

[36] S. Kazemi, Reliability evaluation of smart distribution grids, Ph.D. thesis, Dept. Elect. Eng., Aalto Univ., Espoo, Finland (2011).

[37] Nuuka open api.
URL https://helsinki-openapi.nuuka.cloud/swagger/index.html

[38] Nrel solar radiation database.
URL http://pvwatts.nrel.gov

[39] W. Underground. [link].
URL https://www.wunderground.com

[40] Enercon e44 technical data.
URL https://www.enercon.de/en/products/ep-1/e-44/

[41] Nord pool power market data.
URL https://www.nordpoolgroup.com/Market-data1

[42] Test system details.
URL https://1drv.ms/x/s!AuOkAKT1qZvMyyeDGGRLCM-cT4MK?e=p6raDB